Perfluoroalkyl and polyfluoroalkyl substances (PFAS) in the Yangtze River: Distribution, Transport and Influencing Factors

Xiyan Liu[a], Zhen Zhao [a, b*], Xinyi An [a], Chunhui Wang[a], Chongtai Chen[a], Jing Liu [a], Kevin C. Jones [b], Andrew Sweetman [b], Yan Zeng [c], Tian Lin [a]

[a] College of Oceanography and Ecological Science, Shanghai Ocean University, Shanghai, 201306, China

[b] Lancaster Environment Centre, Lancaster University, Lancaster LA1 4YQ, United Kingdom

[c] State Key Laboratory of Environmental Geochemistry, Institute of Geochemistry, Chinese Academy of Sciences, Guiyang 550002, China

*** Corresponding author:** Zhen Zhao, College of Oceanography and Ecological Science, Shanghai Ocean University, Shanghai 201306, China; Lancaster Environment Centre, Lancaster University, Lancaster LA1 4YQ, United Kingdom

Email: zzhao@shou.edu.cn

Abstract

Per- and polyfluoroalkyl substances (PFAS) are ubiquitous in global river basins. Although the localized influence of the Three Gorges Dam (TGD) on PFAS remobilization is known, a comprehensive investigation of both water and sediment along the entire Yangtze River is lacking. In 2023, 32 PFAS were quantified in water and sediment along over 4000 km of the Yangtze River (China's longest river) and some of its tributaries and nearby lakes. The ∑PFAS concentrations ranged from 5.5 to 340 ng/L in water and 0.13 to 28 ng/g dry weight (dw) in sediments. Higher concentrations were found in water in the preflood period than the postflood period. Notably, short-chain replacement compounds, especially perfluorobutanoic acid (PFBA) and perfluorobutanesulfonate acid (PFBS), dominated the PFAS profile, indicating a compositional shift following legacy homologue restrictions. Spatial analysis revealed elevated concentrations (>100

ng/L) proximate to industrial parks, identifying them as probable point sources. TGD operation created unique hydrological conditions within the Three Gorges Reservoir, resulting in very low PFAS levels (<0.01 ng/g) on suspended particulate matter. Flux calculations indicated that PFAS transportation via the dissolved phase dominated over the particulate phase. Nontarget and suspect screening analysis revealed the occurrence of ultrashort-chain PFAS ($C \leq 3$) in water.

Keywords: Human activities, The three Gorges Dam, Flux, SPM, the Yangtze River

1 Introduction

Perfluoroalkyl and polyfluoroalkyl substances (PFAS) are defined as fluorinated compounds containing at least one fully fluorinated methyl (CF_3-) or methylene (-CF_2-) group, excluding any hydrogen or halogen substitutions.[1] They are widely used in a variety of commercial and consumer products, such as industrial fluoropolymers?, household products, aqueous film-forming foams (AFFF), textiles and non-stick coatings.[2–4] The wide use of PFAS means they have been detected in a variety of media, including air,[5,6] water,[7,8] soil,[9] sediment[10] and aquatic organisms.[11] PFAS exposure has been associated with various toxic effects, including developmental toxicity, genotoxicity, neurotoxicity, and immunotoxicity.[12,13] PFAS, PFOS, PFOA, and PFHxS and related compounds have been listed in Annex B, A, and B of the Stockholm Convention in 2009, 2019, and 2022, respectively. [14–16] Since then, there had been an increase in the production and application of short-chain PFAS (C<8) as replacements,[17] such as perfluorobutanoic acid (PFBA) and perfluorobutane sulfonate acid (PFBS). PFBA was the dominant PFAS? compound in water of the Yellow River in 20XX?, making up 1-45% of the total.[18] In Poyang Lake in 2023, PFBA and PFBS were present at 530 ng/L and 320 ng/L, respectively, accounting for 85% of the ΣPFAS concentrations.[19] In Tangxun Lake sampled in 20XX, PFBA was up to 4770 ng/L, and PFBS was 3660 ng/L due to industrial activities.[20] Besides, more and more ultrashort-chain PFAS (C≤3) were reported using tandem or high-resolution mass spectrometry, and these compounds are now widely distributed in precipitation, surface water and ground water. [21–23]

River water and sediment receives PFAS discharged from industrial and municipal sources and transports them to estuaries and coast.[24] Kurwadkar et al (2022) reviewed the global distribution of PFAS in water, and reported deectable concentrations of PFOA and PFOS in rivers all over the world. [25] Moreover, the numbers of emerging PFAS identified by nontarget and suspected screening

technology were larger in water than other environmental media.[26] In China, Xiaoqing River was severely contaminated with extremely high concentrations up to microgram per liter in water or per gram in sediment, and it had been well studied as a hotspot.[27,28] Discharges from industrial parks were considered as the main sources of PFAS in rivers. [29] Sun et al. (2024) found significantly higher concentrations in industrial park wastewater (10.8 μg/L) than downstream river water of (0.7 μg/L), indicating the waste drainage to the Yangtze River. [30] As hydrophilic contaminants, movement of PFAS is strongly related to hydrological conditions, so the seasonal variation of water volumes could result in changing concentration.[31] Apart from that, suspended particulate matter (SPM) also influences the behavior of PFAS due to their hydrophobicity. Long-chain PFAS have stronger affinity to SPM than short-chain PFs.[32,33]

Many studies have investigated PFAS in water and sediment in the Yangtze River. while also identifying correlations between PFAS levels and water quality parameters.[34] Tan et al. investigated the contribution of tributaries at the boundary between the middle and lower stream of the Yangtze River to the PFAS load in the mainstream.[35] Hua et al. investigated how the water in the middle and lower Yangtze River was affected by the fluorine industry, identifying significantly elevated PFAS concentrations in wastewater treatment plants and industrial areas, with notable seasonal differences in PFAS distribution coefficients between dry and flood seasons.[11] PFAS concentrations and composition showed consistency across surface and bottom sediments, with their spatial distribution being influenced by sediment physicochemical properties.[36]

The Yangtze River is the longest (6300 km) river in China and the third longest in the world.[37] The Yangtze? River basin was densely populated, economically prosperous, with dense shipping lanes and many ports.[38] Pan et al. (2014) revealed the contamination of PFAS in the Yangtze River in 2013, and estimated the annual loading of total PFAS to be20.7 tons. [39] Hua et al. (2023) found the effect of the fluorine industry in the middle and lower Yangtze River.[31]The Three Gorges Dam, located on the Yangtze River, is the largest hydroelectric project in the world, with extensive ecological and environmental impacts on the Yangtze River.[40] The Three Gorges Reservoir's operation mode of “storing clean water and discharging muddy flow” has resulted in distinct changes in pollutant dynamics within the Three Gorges Reservoir (TGR), differing significantly from those in natural rivers.[41] The ecological environment of the TGR has become more fragile compared to natural lakes, due to the impact of high-intensity human activities.[42] Since the operation

of the TGD, the amount of sediment entering the sea from the Yangtze River has been reduced by half.[38] The reduced sediment load after the TDG has resulted in scouring of the riverbed and loosingloss? of fine particle, which were considered as the reason for lower concentrations in the midstream sediment.[43,44]

The latest PFAS contamination data of the whole Yangtze River came from samples collected in 2014 for water and 2019 for sediment, and only 15 compounds (at most) were quantified.[43,44] In 2020, the TDG completed its final construction acceptance, which represented the full completion of its construction. No PFAS data is available yet since the TDG was fully completed. Moreover, little attention has been paid so far to the importance of SPM for transportation. To fill the gaps above, this study was conducted in 20xx and: 1) reports the concentration and composition of thirty-three PFAS in water and sediment from the Yangtze River mainstream, some tributaries and lakes over a distance of xxx km, from xxx to xxx. 2) investigates the spatial and temporal distribution of PFAS in water and sediment and the influence of the TGD 3) estimates surface water transport fluxes of PFAS via the dissolved phase and the SPM for target rivers and lakes.

2 Materials and methods

2.1 Sampling collection

From Sichuan to Shanghai (2913 kilometers), water samples were collected at 55 sites in the dry season (April to June) and at 73 sites in the wet season (September to October), 2023. Figure 1 shows the sampling site map.. Polypropylene bottles (PP, CNW, Germany) were used to store water. Sediment samples were collected at 38 and 51 sites in the dry and wet seasons, respectively. Sediment samples were stored in aluminum foil bags and frozen at -20 °C before extraction. Details of the sampling campaign are shown in Text S1 and Table S1.

2.2 Chemicals and reagents

Quantitation was conducted for thirty-two PFAS. Twelve isotopically labelled compounds were used as internal standards (IS). The injection standard (InjS) was 2H-perfluoro-(1,2-$^{13}C_2$)-2-decenoic acid ($^{13}C_2$-8:2 FTUCA). All standards, with purity > 98%, were obtained from Wellington Laboratories Inc. (Ontario, Canada). Other reagents are listed in Text S2, and detailed information was provided in Table S2.

2.3 Sample preparation

The sample preparation procedures followed those of previous studies.[45,46] One liter water was filtered by glass fiber membranes (47 mm, 0.7 μm pore size, Whatman, Maidstone, UK), which was prebaked at 450°C for 4 hours. The glass fiber filter membrane was washed with methanol to elute PFAS from the particle phase to the dissolved phase.[47] Two nanogram IS was added to the dissolved phase. Solid phase extraction (SPE) was then applied with Oasis WAX cartridges (30 μm, 6 mL, 150 mg, Waters Corporation, Milford, USA). Supelclean Envi-Carb Cartridge (1 mL, 100 mg, Merck, Darmstadt, Germany) was used for purification. The extraction process of PFAS from sediment follows that of Zhong et al..[48] Sediment was freeze-dried for 48 hours to remove water. Then 3.0 g of sediment was weighed into PP centrifuge tubes and spiked with 2 ng IS. Sonication was applied for 15 min with 10 mL 0.2% NH_4OH three times. All the supernatant was collected for purification using Supelclean Envi-Carb Cartridge to remove impurities. Finally, the sample was concentrated to 200 μl under nitrogen. Filters extraction processes were the same as sediment. More detailed information is provided in Text S3.

2.4 Instrumental Analysis

Ultra-high performance liquid chromatography-mass spectrometry (UPLC-MS/MS 8050, Shimadzu, Japan) was utilized for target quantification. Monitoring (MRM) mode with negative electrospray ionization (ESI) was used. A UPLC-Orbitrap MS (Orbitrap Exploris 240, Thermo Fisher Scientific, USA) is used to discover or identify non-target and suspect screening of PFAS. More detailed instrument specifications and information is given in Text S4, and Table S2. S3, and S4.

2.5 Non-target and suspect screening

Forty-two dissolved water samples were selected for non-target and suspect screening. Compound Discoverer 3.3 (CD 3.3) was employed to process raw data to acquire selected spectra, and align retention times using methods published by Zhao et al., (2023) and Li et al., (2022).[49,50] More details are given in Text S5, S6. The relative abundance of non-target compounds, were determined semi-quantitatively (Text S7).

2.6 Partition coefficients

The partition coefficients of PFAS between different phases were calculated as follows:

$$log\mathrm{K_d}=\log\frac{\mathrm{C_{SPM}}}{\mathrm{C_D}}\times 1000 \quad (1)$$

$$log\mathrm{K'_d}=\log\frac{\mathrm{C_{SED}}}{\mathrm{C_D}}\times 1000 \quad (2)$$

Here, $\mathrm{K_d}$ was the coefficient between water and particle phase. $\mathrm{K'_d}$ was between water and sediment; $\mathrm{C_D}$, $\mathrm{C_{SPM}}$ and $\mathrm{C_{SED}}$ represent the PFAS concentrations in the dissolved phase (ng/L), suspended particles (ng/g dw) and sediment (ng/g dw), respectively.

2.7 Flux calculation

The fluxes of PFAS at specific sites were calculated as follows:

$$F_D=C_D\times Q_W\times 10^{-9} \quad (3)$$

$$F_S=\frac{C_{SPM}}{C'}\times Q_S\times 10^{-6} \quad (4)$$

F_D was the monthly PFAS flux in dissolved phase (kg), $\mathrm{Q_W}$ was the monthly water volume ($\mathrm{m^3}$), $F_S$was the monthly PFAS flux in sediment (kg), $C'$was the weight of suspended particles in per liter water (g/L), $Q_S$was the monthly sediment weight (10^4 tonnes). Q_S included the mass of suspended matter and sediment on the river bed. In this study, these two parts were not calculated separately, and Q_S was considered to represent the mass of suspended matter.

2.8 Quality control

The method was verified by adding target PFAS to milli-Q water and quartz sand. Recoveries ranged from 45-145% for the dissolved phase samples and 67-144 % for sediment samples (Table S5). The IS recoveries ranged from 61% ($^{13}C_2$-PFDoA) to 80% ($^{13}C_4$-PFOS) (Table S6). During the whole treatment process, polytetrafluoroethylene (PTFE) materials were avoided. Laboratory method blanks were included for every 10 samples. The calibration curve was set up from 0 to 200 ng/mL with R^2>0.99. During injection, one 200 ng/mL standard was inserted in every 10 samples. Limit of detection (LOD) and limit of quantification (LOQ) were determined as 3 times and 10 times the signal-to-noise ratio, respectively. Concentrations in blank samples were below the detection limit. For statistical analyses, concentrations of PFAS under the LOD were treated as half the LOQ.[48]

3 Result and discussion

3.1 Concentration and composition of PFAS

Concentrations in water for individual sites are shown as the sums of dissolved and particle phases. In the Yangtze River mainstream, ∑PFAS concentrations ranged from 5.5 ng/L to 200 ng/L, with a mean level of 59 ng/L (Table 1 and Figure S1). The lowest concentration of 5.5 ng/L was detected at CJ3, at the confluence of the Yangtze River and the Jialing River in Chongqing City, a site with a large dilution effect.. The highest was found at CJ42 (200 ng/L), located near the Nanjing Chemical Industrial Park (NCIP). NCIP is the second largest petrochemical base in China,[51] and high levels of heavy metals have been reported in the water and sediment of this park.[52] Concentrations of ∑PFAS in five tributaries (Jinsha River, Minjiang River, Hanjiang River, Wujiang River, Jialingjiang River) ranged from 4.9 ng/L to 29 ng/L (mean: 14 ng/L), lower than the mainstream. In three lakes, i.e., Poyang Lake, Dongting Lake, and Taihu Lake, ∑PFAS concentrations ranged from 19 ng/L to 340 ng/L (mean: 110 ng/L), higher than the mainstream and the five tributaries. The highest concentration of 340 ng/L was found at PYH1, the entrance of Poyang Lake to the Yangtze River. Consequently, concentrations downstream near PYH1 were all ranging from 110 ng/L (CJ21) to 170 ng/L (CJ22). PFBA and PFBS were detected in all the samples (Table 1), indicating the wide distribution of these C_4 alternatives to the legacy PFAS. PFBS (mean: 18 ng/L) was the predominant compound, accounting for 4-62% of ∑PFAS concentrations (Figure S2). The next two most abundant compounds were PFOA and PFBA, with mean concentrations of 13 and 8.5 ng/L, respectively.

In sediment, ∑PFAS concentrations ranged from 0.13 to 7.5 ng/g dw, with a mean of 1.5 ng/g dw (Figure S3). PFHpS and PFBS were detected in 99% and 93% samples, respectively (Table 1). PFBA and 8:2 FTSA were predominant compounds, with concentrations of 0.60 and 0.32 ng/g dw, accounting for 29% and 28% of ∑PFAS concentrations (Figure S4).

3.2 Spatial and temporal distribution

In the mainstream, concentrations of ∑PFAS in water were similar for over xxx km between sites CJ2 and CJ19 from 20 ng/L (CJ3) to 60 ng/L (CJ17) in the dry season (Figure S1a). After increasing to 190 ng/L at CJ20, ∑PFAS concentrations then dropped to 64 ng/L at CJ23, and then varied from 38 ng/L to 80 ng/L until CJ36. Site CJ20 was near the Jiujiang Economic Development

Zone in Jiangxi Province. Concentrations were all above 100 ng/L from CJ20 to CJ22. From CJ37 to CJ45, the river was influenced by NCIP, and concentrations changed from 33 ng/L to 200 ng/L. Concentrations then varied between 48 ng/L and 70 ng/L from CJ46 to CJ55, except for a high level of 180 ng/L at CJ50, near Taizhou Gaogang High-tech Industrial Park in Jiangsu Province. In contrast, in the wet season, ∑PFAS concentrations were lower and varied between 5.5 ng/L and 36 ng/L from CJ2 to CJ19 and between 42 ng/L and 87 ng/L from CJ20 to CJ56 (Figure S1b). After the highest concentration of 110 ng/L detected at CJ57, where the Huangpu River water discharged to Yangtze River, ∑PFAS concentrations decreased to 86 ng/L at the estuary. The mean concentration in the dry season was 69 ng/L, higher than flood season of 49 ng/L. As shown in Figure 2-I, at 69% of the sites, ∑PFAS concentrations in the dry season were higher than the flood season. Similar seasonal distributions had been reported for pharmaceutical and personal care products and pentachlorophenol in the Yangtze River.[53,54] In contrast, the mean concentration in the sediment in the dry season was 1.3 ng/g dw, slightly lower than that in the flood season of 2.0 ng/g dw. At 73% of the sites where sediments were collected in both the dry and wet seasons, ∑PFAS concentrations were higher in the wet season than the dry season (Figure 2-II). Sedimentation processes and water column-bottom sediment interactions are influenced by several complicating factors, such as flow rate, riverbed area, as well as reservoir and dam regulation controls.[55] Sedimentation and resuspension has been greatly influenced by the operation of the Three Gorges Dam.. The dam holds more than 70% of the sediment transported by the river above it.[56] Sites CJ5-CJ10 in Three Gorges Reservoir (TGR); their concentrations in the dry season ranged from 0.72 to 3.0 ng/g dw, lower than upstream of the reservoir (4.2 ng/g dw atCJ4). During the dry season, the dam releases water and sediments which were stored from the previous wet season.[57] Concentrations in the TGR therefore represent a mixture of historical sedimentation, due to the operation mode of “storing clean water and discharging muddy flow”.[41] The riverbed downstream of the TGD is seasonally flushed, resulting in the loss of fine particles, which have a strong affinity for organic chemicals.[58,59] This should be the reason that a low concentration of 0.76 ng/g dw was found at CJ12, which was the nearest site downstream of TGD, in the region of riverbed scouring.[57,60] The lowest concentrations in the dry (0.37 ng/g dw) and flood (0.13 ng/g dw) seasons were found at CJ16 located in Wuhan City. In Wuhan, the water surface area accounts for one quarter of the land area, suggesting the strong exchange of water and sediment among rivers and lakes.[61] The highest concentrations in the

dry and wet season were 6.2 ng/g dw and 7.5 ng/g dw, and both were found at site CJ32 at Nanjing City, possibly due to the industrial release. These two big cities (Wuhan and Nanjing) with populations each? over nine million have different sedimentation conditions.

Water from surface, medium and bottom layers of the river water column were collected at 11 sites in the mainstream as shown in Figure S3. Higher concentrations were found in the surface than the medium and bottom water at 3 out of 18 batch samples. Except for these three batch samples, the relative deviations of surface water concentrations and mean values were within 20%. Higher concentrations in surface water than deeper layers had been widely reported in marine area.[62,63] However, inland rivers are interfaced by bank conditions, greater mixing andhuman activities, which will result in greater homogenization with depth. However, for specific compounds, different distribution patterns could be found at the same site. For instance, at CJ12 in the dry season, the concentration of PFBS in the surface layer (12 ng/L) was lower than the bottom layer (20 ng/L), while for HFPO-TA, the surface layer (9.4 ng/L) was higher than the bottom layer (4.0 ng/L).

The distribution among lakes and tributaries were different. In Poyang Lake, higher concentration of 340 ng/L (PYH1) were found at the confluence than inner area (46 ng/L-52 ng/L, PYH2 and PYH3) in dry season. However, in flood season, the concentrations in inner lake were 190 ng/L and 200 ng/L at PYH2 and PYH3, higher than 46 ng/L at PYH1. Dongting Lake presented similar spatial and temporal distribution patterns to Poyang Lake in dry and flood season. The water discharge of Poyang and Dongting Lake in dry season (May 2023) were 1.9×10^{10} m^3 and 2×10^{10} m^3 higher than those in flood season (November, 2023) of 6.9×10^{9} $m^3$and 9.7×10^{9} m^3.[64] These indicated that in dry season, the two lakes supplied water to Yangtze River, and discharge high volume of PFAS into the mainstream, and in flood season, Yangtze River water diluted PFAS at the confluences resulting in lower concentrations than inner lakes. Jinsha River, Minjiang River and Jialing River all showed higher concentrations in downstream than upstream in flood season. However, in Hanjiang River, the concentration at downstream site HJ1 was 14 ng/L, lower than 23 ng/L of upstream of HJ3. The Hanjiang River flows into Yangtze River at Wuhan City which is rich in surface water resource resulting in dilution effect. High concentrations of 130 and 240 ng/L were detected in Taihu Lake. The direct connection between Taihu Lake and Yangtze River is Wangyu River, which is an artificially excavated river with a length of 62 km.[65] Site CJ53 was at the downstream of the confluence of Wangyu and Yangtze River, however, the concentration was 73

ng/L, lower than Taihu Lake. CJ14 was the nearest site of confluence of Dongting Lake and Yangtze River, the concentration of 36 ng/L was comparable with DTH3 of 30 ng/L. Similar distribution was also found at CJ21 (65 ng/L) and PYH1 (46 ng/L), which represented the confluence of Poyang Lake and Yangtze River. At the confluence sites of Minjiang River and Jinsha River (JSJ1, 13 ng/L), Jialing River and Yangtze River (CJ3, 5.5 ng/L), the concentrations were all lower than upstream (MJ1, 29 ng/L, JLJ1, 9.5 ng/L) due to the dilution effect. On the contrary, at CJ5, the confluence of Wujiang River and Yangtze River, the concentration of 20 ng/L was higher than tributary upstream of 9.7 ng/L (WJ1) indicating less contamination in Wujiang River.

3.3 Evidence for changing levels and compositions over time

Comparing with previous investigations conducted in Yangtze River, ∑PFAS concentrations in the dry season in 2023 (20 ng/L-200 ng/L) were higher than 2014 (0.30 ng/L-88.50 ng/L), although much of this difference is because this study had more target compounds.[66] However, in the flood season, ∑PFAS concentrations were comparable ranging from ND-69 ng/L in 2014 and 5.5-87 ng/L in 2023.[34] Between CJ11 and CJ17, ∑PFAS concentrations in 2023 were 21-36 ng/L, lower than the 12-77 ng/L detected in 2018.[67] Samples collected in Nanjing City (CJ36-CJ38) had comparable concentrations in both the dry (53-110 ng/L) and flood (48-58 ng/L) seasons, with those detected in 2017 (25-100 ng/L, dry season) and 2018 (0.8-40 ng/L, flood season). Regarding the mixture of PFAS, PFOA was the dominant compound in studies conducted in 2014 and 2017. However, PFBS (18 ng/L) was the predominant compound in this study. The contribution of PFBS (8 - 66%) in this study was higher than in 2014 (0.32-50%), suggesting that short-chain PFAS are now more? widely used as substitutes for long-chain PFAS.[68] In addition, HFPO-TA (2.7 ng/L) was the most prominent emerging PFAS; it is now used as an alternative to ??.[69] High concentrations of PFHxA were found in 2018 (0.66 -31 ng/L) and 2020/2021 (1.0 -465 ng/L). However, in this study, PFHxA concentrations varied from 0.23 to 40 ng/L, with a mean concentration of 5.2 ng/L. Comparing more widely, the mean concentration in the Yangtze River (59 ng/L) in this study was higher than reported in other Chinese rivers, (e.g. Pearl River (19 ng/L),[70] Hai River (27 ng/L),[71] and Yellow River (24 ng/L)),[72] the River Seine (27 ng/L) in France,[73] and the River Rhine (33 ng/L) in Germany.[74] However, it was lower than the Yongsan River (94 ng/L) in Korea and the Qiantang River (150 ng/L) in China.[75,76]

In sediment, ∑PFAS concentrations (2.0 ng/g dw) in 2023 were higher than 2024 (0.19 ng/g

dw).[36] PFBA and PFBS were predominant, ranging from <LOQ to 2.6 ng/g dw and <LOQ to 1.6 ng/g dw, respectively. Moreover, PFBA and PFBS contributed 15% and 7% of ∑PFAS respectively. Although PFOA (59%) and PFOS (59%) were detected at higher rates than PFBA (38%). This is contrary to the study of Li et al..[36] Comparing with other rivers worldwide, the mean ∑PFAS concentration in this study (3.9 ng/g dw) was higher than the Namhan River (0.39 ng/g dw), Bukhan River (0.25 ng/g dw), Nakdong River (0.43 ng/g dw), Nam River (0.35 ng/g dw) and Yeongsan River (0.35 ng/g dw) in Korea,[77] as well as across Vietnam (1.1 ng/g dw).[78] However, it was lower than concentrations found in the Truckee River (21 ng/g dw) andLas Vegas Wash (29 ng/g dw) in America,[79] and the River Orge (29 ng/g dw) in France.[80]

3.4 Partitioning behavior

Log K_d and log K'_d were calculated for detected PFAS compounds (Table S9). In the dry season, the individual mean value of log K_d and log K'_d ranged between 0.56-3.1 and 0.41-3.9, respectively. In the wet season, mean log K_d ranged between 0.27-4.5 and 0.85-4.0 for log K'_d. These values are comparable to the River Orge (log K_d: 1.6-5.0) in France,[80] Tokyo Bay (log K_d: 1.9-4.2) in Japan [81] and Jiulong Estuary-Xiamen Bay (log K'_d: 1.6-4.1) in China [82]. Log K_d and log K'_d values increased with increasing carbon chain lengths (seeing Figure 3). HFPO-TA had comparable log K_d (1.80) and log K'_d values (1.54) to PFOS (log K_d 1.47, and log K'_d 1.74), and they were all lower than those of PFECHS (log K_d 2.53, and log K'_d 2.48). K_d and K'_d are influenced by a variety of factors e.g. temperature, ionic strength, organic matter content and hydrogeological conditions.[82,83]

3.5 Transport fluxes

The ∑PFAS fluxes in the sampling months are presented in Table 2. F_D values were higher than F_S at all sites, indicating that transportation in the dissolved phase dominated. However, transport with the suspended matter could not be ignored, contributing between <1-47%. F_D generally increased from upstream (CJ2) to downstream (CJ25/CJ53), while F_S varied due to human activities. Above the Three Gorges reservoir, F_S were 220 kg and 240 kg at CJ2 and 99 kg at CJ3, and the contributions of suspended matter were 26-38%. Below the Three Gorges dam, F_S decreased dramatically to 49 kg (at CJ11), and 24 kg (dry season) and 68 kg (flood season) at CJ13; the proportion on suspended particles dropped to 2-6%. Interestingly, in the dry season, Q_S values were 20 t at CJ2, and 10 t and 30 t at CJ11 and CJ13. Both these sites are in the riverbed scour area. This phenomenon was consistent to distribution of PFAS in sediment meaning that suspended matter as

well as riverbed sediment in scour area were loaded less PFAS due to coarse particles. CJ16 is downstream of the riverbed scour area. Here, the percentage of F_S was 30% (520 kg) in the dry season and 10% (170 kg) in the flood season. F_D values at the same sites in different seasons were comparable; for instance, at CJ13 F_D in both the dry and wet seasons were 1100 kg, even though the concentrations and water volumes were different. This meant that the dam, which controls the water runoff, kept the contaminant fluxes consistent. As for F_S, the values in the wet season were higher than the dry season at CJ2 and CJ13. After the riverbed scour area, F_S values in the dry season were higher at CJ16 and CJ25.

At MJ1, the F_D and F_S values were all higher than the downstream site JSJ1, due to the high concentrations of ∑PFAS. However, the contributions of suspended matter were 1%. Dongting and Poyang Lake both supply water and suspended matter to the Yangtze River? in the dry season, and F_D and F_S values in these two lakes were higher in the dry season than the flood season. Differently, F_D values at PYH1 in both seasons were higher than DTH1, but F_S values presented the opposite pattern, indicating Poyang Lake discharge more PFAS through dissolved phase, while Dongting Lake discharge more through suspended matter.

In this study, the suspended matter was assumed to represent the whole part of transportable sediment which introduced uncertainty of the flux calculation. To our best knowledge, the specific proportion of suspended matter to transportable sediment could not be found. Glass fiber filter membranes were rinsed with methanol during the pretreatment. A part of the particle phase was washed to the dissolved phase. The flux of PFAS in the particle phase was therefore underestimated. In summary, this study demonstrates that the contribution of SPM to the transport of PFAS should be considered.

3.6 Semi-quantified compounds

Seven compounds were identified by nontarget and suspect screening,. These weretrifluoroacetic acid (TFA), perfluoropropionic acid (PFPrA), trifluoromethanesulfonic acid (TFMS), perfluorooctanesulfonic acid (PFPrS), N-methylperfluorooctane sulfonamidoacetic acid (N-MeFBSAA), hexafluorobutylene sulfone (H-PFBS), and heptafluoropropyl acrylate (H-PFPrA). Five of them were ultrashort-chain PFAS (C≤3). The raw semi-quantitative data for 38 samples at 30 sites are shown in Table S16 and Figure 4. The semi-quantitative method was described in Text S7. The concentration of ∑PFAS ranged from 0.010 ng/L to 48 ng/L (mean:10 ng/L). The mean

concentrations of TFA and PFPrA were 3.7 ng/L and 3.9 ng/L, accounting for 38% and 34% of total concentrations, respectively. TFA is a degradation product of certain PFAS, pharmaceuticals and pesticides, as well as photodegradation products of refrigerants, gas extinguishing and foaming agents.[84] It had been widely reported in surface waters, waste water and precipitation.[85–87] PFPrA has similar sources to TFA, however, it concentrations were lower than TFA in previous studies.[88,89] Higher ∑PFAS concentrations of 15-21 ng/L were found at CJ42, 44, and 45, close to the NICP. This was consistent with the results of target PFAS. Poyang Lake also showed high concentrations of 48 ng/L in the dry season and 39 ng/L in wet season. PFAS has been reported at high levels in wastes, sediment, and biota from Poyang Lake.[90–92] However, this is the first report of ultrashort-chain PFAS in Poyang Lake.

4 Conclusions

~~This~~ study investigated the spatial and temporal distribution of PFAS in water and sediment from Yangtze River mainstem with a length of over 5000 km, four tributaries and three lakes. The ΣPFAS concentrations in Jinsha River (the name of upstream of Yangtze River) and Yangtze River mainstem were 5.5 to 200 ng/L in water and 0.13 to 7.5 ng/g dw in sediments. The highest ΣPFAS concentration of 340 ng/L in water was detected in dry season in Poyang Lake which discharge PFAS into Yangtze River. In the sites which samples were collected both in dry and flood season, 69% paired water samples exhibited higher ΣPFAS concentration in dry than flood season, while 73% paired sediment samples showed higher concentration in flood season. The variations between surface and mean values of different layers were less than 20% in 16 out of 18 batch samples. High ΣPFAS concentrations over 100 ng/L were detect near industrial parks in Jiujiang, Nanjing, Taizhou, and Shanghai. The operation of the TGD influenced the distribution of PFAS in sediments in the TGR and riverbed scour area. Moreover, the PFAS fluxes transported via SPM were 26% to 38% before the Three Gorgers Dam (CJ2-CJ3), and decreased to 2% to 6% in riverbed scour area. PFAS transportation via dissolved phase accounted for 53% to >99% of total fluxes, however, the contribution of SPM could not be overlooked. Severn emerging PFAS were identified through nontarget and suspect screening analysis. TFA and PFPrA accounted for 38% and 34% of semi-quantified total PFAS concentrations. This study revealed the influence of human activities on PFAS distribution and the importance of SPM for PFAS transportation.

CRediT author statement

Zhen Zhao: Conceptualization, Writing - review & editing, Supervision, Resources, Funding acquisition. **Xinyi An**: Methodology, Software, Writing - original draft, Formal analysis, Data curation. **Chunhui Wang**: Investigation, Data curation. **Chongtai Chen**: Investigation, Formal analysis. **Jing Liu**: Software, Data Curation. **Kevin C. Jones**: Writing - review & editing, Formal analysis. **Andrew Sweetman**: Writing - review & editing. **Yan Zeng**: Project administration. **Tian Lin**: Resources, Project administration, Funding acquisition.

Declaration of Competing Interest

The authors declare that they have no known competing financial interests or personal relationships that could have appeared to influence the work reported in this paper.

Data Availability

Data will be made available on request.

Acknowledgments

This research was funded by the National Key Research and Development Program of China (No. 2021YFC3201002), the National Natural Science Foundation of China (No. 41977310) and the China Scholarship Council (CSC) Program for Senior Research Scholars, Visiting Scholars and Postdoctoral Researchers. The authors would like to acknowledge the sampling staff and all colleagues who helped in the experimental and writing process.

Reference:

(1) *ECHA, 2023*. https://echa.europa.eu/pfas-restriction (accessed 2025-01-27).

(2) Buck, R. C.; Korzeniowski, S. H.; Laganis, E.; Adamsky, F. Identification and Classification of Commercially Relevant Per- and Poly-Fluoroalkyl Substances (PFAS). *Integrated Environmental Assessment and Management* **2021**, *17* (5), 1045–1055. https://doi.org/10.1002/ieam.4450.

(3) Chen, Y.; Wei, L.; Luo, W.; Jiang, N.; Shi, Y.; Zhao, P.; Ga, B.; Pei, Z.; Li, Y.; Yang, R.; Zhang, Q. Occurrence, Spatial Distribution, and Sources of PFASs in the Water and Sediment from Lakes in the Tibetan Plateau. *Journal of Hazardous Materials* **2023**, *443*, 130170. https://doi.org/10.1016/j.jhazmat.2022.130170.

(4) Macorps, N.; Labadie, P.; Lestremau, F.; Assoumani, A.; Budzinski, H. Per- and Polyfluoroalkyl Substances (PFAS) in Surface Sediments: Occurrence, Patterns, Spatial Distribution and Contribution of Unattributed Precursors in French Aquatic Environments. *Science of The Total Environment* **2023**, *874*, 162493. https://doi.org/10.1016/j.scitotenv.2023.162493.

(5) Fang, S.; Li, C.; Zhu, L.; Yin, H.; Yang, Y.; Ye, Z.; Cousins, I. T. Spatiotemporal Distribution and Isomer Profiles of Perfluoroalkyl Acids in Airborne Particulate Matter in Chengdu City, China. *Science of The Total Environment* **2019**, *689*, 1235–1243. https://doi.org/10.1016/j.scitotenv.2019.06.498.

(6) Tian, Y.; Yao, Y.; Chang, S.; Zhao, Z.; Zhao, Y.; Yuan, X.; Wu, F.; Sun, H. Occurrence and Phase Distribution of Neutral and Ionizable Per- and Polyfluoroalkyl Substances (PFASs) in the Atmosphere and Plant Leaves around Landfills: A Case Study in Tianjin, China. *Environ. Sci. Technol.* **2018**, *52* (3), 1301–1310. https://doi.org/10.1021/acs.est.7b05385.

(7) Hua, Z.; Yu, L.; Liu, X.; Zhang, Y.; Ma, Y.; Lu, Y.; Wang, Y.; Yang, Y.; Xue, H. Perfluoroalkyl Acids in Surface Sediments from the Lower Yangtze River: Occurrence, Distribution, Sources, Inventory, and Risk Assessment. *Science of The Total Environment* **2021**, *798*, 149332. https://doi.org/10.1016/j.scitotenv.2021.149332.

(8) Podder, A.; Sadmani, A. H. M. A.; Reinhart, D.; Chang, N.-B.; Goel, R. Per and Poly-Fluoroalkyl Substances (PFAS) as a Contaminant of Emerging Concern in Surface Water: A Transboundary Review of Their Occurrences and Toxicity Effects. *Journal of Hazardous Materials* **2021**, *419*, 126361. https://doi.org/10.1016/j.jhazmat.2021.126361.

(9) Brusseau, M. L.; Anderson, R. H.; Guo, B. PFAS Concentrations in Soils: Background Levels versus Contaminated Sites. *Science of The Total Environment* **2020**, *740*, 140017. https://doi.org/10.1016/j.scitotenv.2020.140017.

(10) Mussabek, D.; Ahrens, L.; Persson, K. M.; Berndtsson, R. Temporal Trends and Sediment–Water Partitioning of per- and Polyfluoroalkyl Substances (PFAS) in Lake Sediment. *Chemosphere* **2019**, *227*, 624–629. https://doi.org/10.1016/j.chemosphere.2019.04.074.

(11) Hua, Z.; Gao, C.; Zhang, J.; Li, X. Perfluoroalkyl Acids in the Aquatic Environment of a Fluorine Industry-Impacted Region: Spatiotemporal Distribution, Partition Behavior, Source, and Risk Assessment. *Science of The Total Environment* **2023**, *857*, 159452. https://doi.org/10.1016/j.scitotenv.2022.159452.

(12) Fenton, S. E.; Ducatman, A.; Boobis, A.; DeWitt, J. C.; Lau, C.; Ng, C.; Smith, J. S.; Roberts, S. M. Per- and Polyfluoroalkyl Substance Toxicity and Human Health Review:

Current State of Knowledge and Strategies for Informing Future Research. *Enviro Toxic and Chemistry* **2021**, *40* (3), 606–630. https://doi.org/10.1002/etc.4890.

(13) Singh, N.; Hsieh, C. Y. J. Exploring Potential Carcinogenic Activity of Per- and Polyfluorinated Alkyl Substances Utilizing High-Throughput Toxicity Screening Data. *Int J Toxicol* **2021**, *40* (4), 355–366. https://doi.org/10.1177/10915818211010490.

(14) UNEP. Provisional Health Advisories for Perfluorooctanoic Acid (PFOA) and Perfluorooctane Sulfonate (PFOS). **2009**.

(15) *UNEP 2022 In Listing PFHxS, its salts and PFHxS-related compounds in Annex A to the Stockholm Convention (decision SC-10/13)*. https://www.unep.org/news-and-stories/press-release/brs-cops-conclude-major-decisions-e-waste-movement-and-ban-harmful (accessed 2025-02-13).

(16) *UNEP, 2019a. listing of perfluorooctanoic acid (2019), its salts and PFOA-related compounds. SC-9/12*.

(17) Lim, X. Tainted Water: The Scientists Tracing Thousands of Fluorinated Chemicals in Our Environment. *Nature* **2019**, *566* (7742), 26–30.

(18) Wang, P.; Lu, Y.; Wang, T.; Fu, Y.; Zhu, Z.; Liu, S.; Xie, S.; Xiao, Y.; Giesy, J. P. Occurrence and Transport of 17 Perfluoroalkyl Acids in 12 Coastal Rivers in South Bohai Coastal Region of China with Concentrated Fluoropolymer Facilities. *Environmental Pollution* **2014**, *190*, 115–122. https://doi.org/10.1016/j.envpol.2014.03.030.

(19) Tang, A.; Zhang, X.; Li, R.; Tu, W.; Guo, H.; Zhang, Y.; Li, Z.; Liu, Y.; Mai, B. Spatiotemporal Distribution, Partitioning Behavior and Flux of per- and Polyfluoroalkyl Substances in Surface Water and Sediment from Poyang Lake, China. *Chemosphere* **2022**, *295*, 133855. https://doi.org/10.1016/j.chemosphere.2022.133855.

(20) Zhou, Z.; Liang, Y.; Shi, Y.; Xu, L.; Cai, Y. Occurrence and Transport of Perfluoroalkyl Acids (PFAAs), Including Short-Chain PFAAs in Tangxun Lake, China. *Environ. Sci. Technol.* **2013**, *47* (16), 9249–9257. https://doi.org/10.1021/es402120y.

(21) Gorji, S. G.; Ramos, M. J. G.; Dewapriya, P.; Schulze, B.; Mackie, R.; Nguyen, T. M. H.; Higgins, C. P.; Bowles, K.; Mueller, J. F.; Thomas, K. V.; Kaserzon, S. L. New PFASs Identified in AFFF Impacted Groundwater by Passive Sampling and Nontarget Analysis. *ENVIRONMENTAL SCIENCE & TECHNOLOGY* **2024**, *58* (3), 1690–1699. https://doi.org/10.1021/acs.est.3c06591.

(22) Freeling, F.; Behringer, D.; Heydel, F.; Scheurer, M.; Ternes, T. A.; Nödler, K. Trifluoroacetate in Precipitation: Deriving a Benchmark Data Set. *Environ. Sci. Technol.* **2020**, *54* (18), 11210–11219. https://doi.org/10.1021/acs.est.0c02910.

(23) Wang, Q.; Ruan, Y.; Yuen, C. N. T.; Lin, H.; Yeung, L. W. Y.; Leung, K. M. Y.; Lam, P. K. S. Tracing Per- and Polyfluoroalkyl Substances (PFASs) in the Aquatic Environment: Target Analysis and Beyond. *TrAC Trends in Analytical Chemistry* **2023**, *169*, 117351. https://doi.org/10.1016/j.trac.2023.117351.

(24) Anik, A. H.; Basir, Md. S.; Sultan, M. B.; Alam, M.; Rahman, Md. M.; Tareq, S. M. Unveiling the Emerging Concern of Per- and Polyfluoroalkyl Substances (PFAS) and Their Potential Impacts on Estuarine Ecosystems. *Marine Pollution Bulletin* **2025**, *212*, 117554. https://doi.org/10.1016/j.marpolbul.2025.117554.

(25) Kurwadkar, S.; Dane, J.; Kanel, S. R.; Nadagouda, M. N.; Cawdrey, R. W.; Ambade, B.; Struckhoff, G. C.; Wilkin, R. Per- and Polyfluoroalkyl Substances in Water and

Wastewater: A Critical Review of Their Global Occurrence and Distribution. *Science of The Total Environment* **2022**, *809*, 151003. https://doi.org/10.1016/j.scitotenv.2021.151003.

(26) Ng, K.; Alygizakis, N.; Androulakakis, A.; Galani, A.; Aalizadeh, R.; Thomaidis, N. S.; Slobodnik, J. Target and Suspect Screening of 4777 Per- and Polyfluoroalkyl Substances (PFAS) in River Water, Wastewater, Groundwater and Biota Samples in the Danube River Basin. *Journal of Hazardous Materials* **2022**, *436*, 129276. https://doi.org/10.1016/j.jhazmat.2022.129276.

(27) Colomer-Vidal, P.; Jiang, L.; Mei, W.; Luo, C.; Lacorte, S.; Rigol, A.; Zhang, G. Plant Uptake of Perfluoroalkyl Substances in Freshwater Environments (Dongzhulong and Xiaoqing Rivers, China). *Journal of Hazardous Materials* **2022**, *421*, 126768. https://doi.org/10.1016/j.jhazmat.2021.126768.

(28) Tulcan, R. X. S.; Yarleque, C. M. H.; Lu, X.; Yeerkenbieke, G.; Herrera, V. O.; Gunarathne, V.; Yánez-Jácome, G. S. Characterization of Per- and Polyfluoroalkyl Substances (PFASs) in Chinese River and Lake Sediments. *Journal of Hazardous Materials* **2025**, *489*, 137680. https://doi.org/10.1016/j.jhazmat.2025.137680.

(29) Yu, L.; Hua, Z.; Liu, X.; Xing, X.; Zhang, C.; Hu, T.; Xue, H. Multi-Compartment Levels and Distributions of per- and Polyfluoroalkyl Substances Surrounding Fluorochemical Manufacturing Parks in China: A Review of the Current Literature. *Journal of Hazardous Materials* **2024**, *480*, 136196. https://doi.org/10.1016/j.jhazmat.2024.136196.

(30) Sun, S.; Liang, M.; Fan, D.; Gu, W.; Wang, Z.; Shi, L.; Geng, N. Occurrence and Profiles of Perfluoroalkyl Substances in Wastewaters of Chemical Industrial Parks and Receiving River Waters: Implications for the Environmental Impact of Wastewater Discharge. *Science of The Total Environment* **2024**, *945*, 173993. https://doi.org/10.1016/j.scitotenv.2024.173993.

(31) Hua, Z.; Gao, C.; Zhang, J.; Li, X. Perfluoroalkyl Acids in the Aquatic Environment of a Fluorine Industry-Impacted Region: Spatiotemporal Distribution, Partition Behavior, Source, and Risk Assessment. *Science of The Total Environment* **2023**, *857*, 159452. https://doi.org/10.1016/j.scitotenv.2022.159452.

(32) Munoz, G.; Budzinski, H.; Babut, M.; Lobry, J.; Selleslagh, J.; Tapie, N.; Labadie, P. Temporal Variations of Perfluoroalkyl Substances Partitioning between Surface Water, Suspended Sediment, and Biota in a Macrotidal Estuary. *Chemosphere* **2019**, *233*, 319–326. https://doi.org/10.1016/j.chemosphere.2019.05.281.

(33) Göckener, B.; Fliedner, A.; Rüdel, H.; Badry, A.; Koschorreck, J. Long-Term Trends of Per- and Polyfluoroalkyl Substances (PFAS) in Suspended Particular Matter from German Rivers Using the Direct Total Oxidizable Precursor (dTOP) Assay. *Environ. Sci. Technol.* **2022**, *56* (1), 208–217. https://doi.org/10.1021/acs.est.1c04165.

(34) Pan, C.-G.; Ying, G.-G.; Zhao, J.-L.; Liu, Y.-S.; Jiang, Y.-X.; Zhang, Q.-Q. Spatiotemporal Distribution and Mass Loadings of Perfluoroalkyl Substances in the Yangtze River of China. *Science of The Total Environment* **2014**, *493*, 580–587. https://doi.org/10.1016/j.scitotenv.2014.06.033.

(35) Tan, K.-Y.; Lu, G.-H.; Yuan, X.; Zheng, Y.; Shao, P.-W.; Cai, J.-Y.; Zhao, Y.-R.; Zhu, X.-H.; Yang, Y.-L. Perfluoroalkyl Substances in Water from the Yangtze River and Its Tributaries at the Dividing Point Between the Middle and Lower Reaches. *Bull Environ Contam Toxicol* **2018**, *101* (5), 598–603. https://doi.org/10.1007/s00128-018-2444-z.

(36) Li, T.; Chen, Y.; Wang, Y.; Tan, Y.; Jiang, C.; Yang, Y.; Zhang, Z. Occurrence, Source Apportionment and Risk Assessment of Perfluorinated Compounds in Sediments from the Longest River in Asia. *Journal of Hazardous Materials* **2024**, *467*, 133608. https://doi.org/10.1016/j.jhazmat.2024.133608.

(37) Tang, Z.; Yang, Z.; Shen, Z.; Niu, J.; Cai, Y. Residues of Organochlorine Pesticides in Water and Suspended Particulate Matter from the Yangtze River Catchment of Wuhan, China. *Environ Monit Assess* **2008**, *137* (1–3), 427. https://doi.org/10.1007/s10661-007-9778-z.

(38) Xiaohe Lai. *The process and mechanism of river channel erosion below Three Gorges Dam-its effect and prediction to sediment load into the sea*.

(39) Pan, C.-G.; Ying, G.-G.; Zhao, J.-L.; Liu, Y.-S.; Jiang, Y.-X.; Zhang, Q.-Q. Spatiotemporal Distribution and Mass Loadings of Perfluoroalkyl Substances in the Yangtze River of China. *Science of The Total Environment* **2014**, *493*, 580–587. https://doi.org/10.1016/j.scitotenv.2014.06.033.

(40) Xiong, Y. J.; Yin, J.; Paw U, K. T.; Zhao, S. H.; Qiu, G. Y.; Liu, Z. How the Three Gorges Dam Affects the Hydrological Cycle in the Mid-Lower Yangtze River: A Perspective Based on Decadal Water Temperature Changes. *Environ. Res. Lett.* **2020**, *15* (1), 014002. https://doi.org/10.1088/1748-9326/ab5d9a.

(41) He Ruiting; Yang Kang; Zeng Bo; Li Rui; Niu Hangang; Shi Shaohua; Ayi Qiaoli; Su Xiaolei. Distribution pattern of vegetation in water-level fluctuation zone of the Three Gorges Reservoir as affected by differential flooding regimes. *Acta Ecologica Sinica* **2020**, *40* (3). https://doi.org/10.5846/stxb201811032382.

(42) Zhang, S.; Li, X.; He, D.; Zhang, D.; Zhao, Z.; Si, H.; Wang, F. Per- and Poly-Fluoroalkyl Substances in Sediments from the Water-Level-Fluctuation Zone of the Three Gorges Reservoir, China: Contamination Characteristics, Source Apportionment, and Mass Inventory and Loadings. *Environmental Pollution* **2022**, *299*, 118895. https://doi.org/10.1016/j.envpol.2022.118895.

(43) Li, J.; Gao, Y.; Xu, N.; Li, B.; An, R.; Sun, W.; Borthwick, A. G. L.; Ni, J. Perfluoroalkyl Substances in the Yangtze River: Changing Exposure and Its Implications after Operation of the Three Gorges Dam. *Water Research* **2020**, *182*, 115933. https://doi.org/10.1016/j.watres.2020.115933.

(44) Li, T.; Chen, Y.; Wang, Y.; Tan, Y.; Jiang, C.; Yang, Y.; Zhang, Z. Occurrence, Source Apportionment and Risk Assessment of Perfluorinated Compounds in Sediments from the Longest River in Asia. *Journal of Hazardous Materials* **2024**, *467*, 133608. https://doi.org/10.1016/j.jhazmat.2024.133608.

(45) Cai, Y.; Wang, X.; Wu, Y.; Zhao, S.; Li, Y.; Ma, L.; Chen, C.; Huang, J.; Yu, G. Temporal Trends and Transport of Perfluoroalkyl Substances (PFASs) in a Subtropical Estuary: Jiulong River Estuary, Fujian, China. *Science of The Total Environment* **2018**, *639*, 263–270. https://doi.org/10.1016/j.scitotenv.2018.05.042.

(46) Liu, J.; Zhao, Z.; Li, J.; Hua, X.; Zhang, B.; Tang, C.; An, X.; Lin, T. Emerging and Legacy Perfluoroalkyl and Polyfluoroalkyl Substances (PFAS) in Surface Water around Three International Airports in China. *Chemosphere* **2023**, 140360. https://doi.org/10.1016/j.chemosphere.2023.140360.

(47) Liu, S.; Jin, B.; Arp, H. P. H.; Chen, W.; Liu, Y.; Zhang, G. The Fate and

Transport of Chlorinated Polyfluorinated Ether Sulfonates and Other PFAS through Industrial Wastewater Treatment Facilities in China. *Environ. Sci. Technol.* **2022**, *56* (5), 3002–3010. https://doi.org/10.1021/acs.est.1c04276.

(48) Zhong, H.; Zheng, M.; Liang, Y.; Wang, Y.; Gao, W.; Wang, Y.; Jiang, G. Legacy and Emerging Per- and Polyfluoroalkyl Substances (PFAS) in Sediments from the East China Sea and the Yellow Sea: Occurrence, Source Apportionment and Environmental Risk Assessment. *Chemosphere* **2021**, *282*, 131042. https://doi.org/10.1016/j.chemosphere.2021.131042.

(49) Zhao, M.; Yao, Y.; Dong, X.; Baqar, M.; Fang, B.; Chen, H.; Sun, H. Nontarget Identification of Novel Per- and Polyfluoroalkyl Substances (PFAS) in Soils from an Oil Refinery in Southwestern China: A Combined Approach with TOP Assay. *Environ. Sci. Technol.* **2023**, *57* (48), 20194–20205. https://doi.org/10.1021/acs.est.3c05859.

(50) Li, L.; Yu, N.; Wang, X.; Shi, W.; Liu, H.; Zhang, X.; Yang, L.; Pan, B.; Yu, H.; Wei, S. Comprehensive Exposure Studies of Per- and Polyfluoroalkyl Substances in the General Population: Target, Nontarget Screening, and Toxicity Prediction. *Environ. Sci. Technol.* **2022**, *56* (20), 14617–14626. https://doi.org/10.1021/acs.est.2c03345.

(51) Zhen, X. L.; Liu, G.; Li, J. H.; Xu, H.; Wu, D. PAHs in Road Dust of Nanjing Chemical Industry Park, China: Chemical Composition, Sources, and Risk Assessment. *JOURNAL OF ENVIRONMENTAL SCIENCE AND HEALTH PART A-TOXIC/HAZARDOUS SUBSTANCES & ENVIRONMENTAL ENGINEERING* **2020**, *55* (1), 33–43. https://doi.org/10.1080/10934529.2019.1667166.

(52) Cheng, J.; Shen, M.; Wu, J.; Zhao, Z.; Mao, L.; Gao, S. DISTRIBUTION AND ASSESSMENT OF HEAVY METALS IN SURFACE WATER AND SEDIMENTS FROM NANJING CHEMICAL INDUSTRIAL PARK. *FRESENIUS ENVIRONMENTAL BULLETIN* **2012**, *21* (9A), 2702–2710.

(53) Yang, F.; Wan, Y.; Wang, Y.; Li, S.; Xu, S.; Xia, W. Occurrence of Pentachlorophenol in Surface Water from the Upper to Lower Reaches of the Yangtze River and Treated Water in Wuhan, China. *ENVIRONMENTAL SCIENCE AND POLLUTION RESEARCH* **2024**. https://doi.org/10.1007/s11356-024-32821-0.

(54) Yin, C.; Tan, Y.; Chen, Y.; Gao, S.; Wu, M.; Zhang, Z. Mass Load and Source Apportionment of Pharmaceutical and Personal Care Product in the Wuhan Section of the Yangtze River, China. *The Science of the total environment* **2025**, *959*, 178222–178222. https://doi.org/10.1016/j.scitotenv.2024.178222.

(55) Xu, K.; Milliman, J. D. Seasonal Variations of Sediment Discharge from the Yangtze River before and after Impoundment of the Three Gorges Dam. *GEOMORPHOLOGY* **2009**, *104* (3–4), 276–283. https://doi.org/10.1016/j.geomorph.2008.09.004.

(56) Yang, Y.; Zheng, J.; Zhu, L.; Zhang, H.; Wang, J. Influence of the Three Gorges Dam on the Transport and Sorting of Coarse and Fine Sediments Downstream of the Dam. *JOURNAL OF HYDROLOGY* **2022**, *615*. https://doi.org/10.1016/j.jhydrol.2022.128654.

(57) Lai, Xiaohe. The Process and Mechanism of River Channel Erosion Below Three Gorges Dam-Its Effect and Prediction to Sediment Load into the Sea. Doctoral Dissertations, East China Normal University, 2018.

(58) Munoz, G.; Budzinski, H.; Labadie, P. Influence of Environmental Factors on

the Fate of Legacy and Emerging Per- and Polyfluoroalkyl Substances along the Salinity/Turbidity Gradient of a Macrotidal Estuary. *ENVIRONMENTAL SCIENCE & TECHNOLOGY* **2017**, *51* (21), 12347–12357. https://doi.org/10.1021/acs.est.7b03626.

(59) Yang, Y.; Zheng, J.; Zhu, L.; Zhang, H.; Wang, J. Influence of the Three Gorges Dam on the Transport and Sorting of Coarse and Fine Sediments Downstream of the Dam. *JOURNAL OF HYDROLOGY* **2022**, *615*. https://doi.org/10.1016/j.jhydrol.2022.128654.

(60) Guo, L.; Su, N.; Zhu, C.; He, Q. How Have the River Discharges and Sediment Loads Changed in the Changjiang River Basin Downstream of the Three Gorges Dam? *JOURNAL OF HYDROLOGY* **2018**, *560*, 259–274. https://doi.org/10.1016/j.jhydrol.2018.03.035.

(61) Wuhan Municipal Water Affairs Bureau. *Wuhan on the Yangtze River*. https://swj.wuhan.gov.cn/mlsw/.

(62) Brumovsky, M.; Karaskova, P.; Borghini, M.; Nizzetto, L. Per- and Polyfluoroalkyl Substances in the Western Mediterranean Sea Waters. *CHEMOSPHERE* **2016**, *159*, 308–316. https://doi.org/10.1016/j.chemosphere.2016.06.015.

(63) Miranda, D. de A.; Leonel, J.; Benskin, J. P.; Johansson, J.; Hatje, V. Perfluoroalkyl Substances in the Western Tropical Atlantic Ocean. *ENVIRONMENTAL SCIENCE & TECHNOLOGY* **2021**, *55* (20), 13749–13758. https://doi.org/10.1021/acs.est.1c01794.

(64) *Changjiang Water Resources Commission of the Ministry of Water Resources*. http://www.cjw.gov.cn/ (accessed 2025-02-14).

(65) Yao, J.; Sheng, N.; Guo, Y.; Yeung, L. W. Y.; Dai, J.; Pan, Y. Nontargeted Identification and Temporal Trends of Per- and Polyfluoroalkyl Substances in a Fluorochemical Industrial Zone and Adjacent Taihu Lake. *ENVIRONMENTAL SCIENCE & TECHNOLOGY* **2022**, *56* (12), 7986–7996. https://doi.org/10.1021/acs.est.2c00891.

(66) Li, J.; Gao, Y.; Xu, N.; Li, B.; An, R.; Sun, W.; Borthwick, A. G. L.; Ni, J. Perfluoroalkyl Substances in the Yangtze River: Changing Exposure and Its Implications after Operation of the Three Gorges Dam. *Water Research* **2020**, *182*, 115933. https://doi.org/10.1016/j.watres.2020.115933.

(67) Pan, Y.; Zhang, H.; Cui, Q.; Sheng, N.; Yeung, L. W. Y.; Sun, Y.; Guo, Y.; Dai, J. Worldwide Distribution of Novel Perfluoroether Carboxylic and Sulfonic Acids in Surface Water. *Environ. Sci. Technol.* **2018**, *52* (14), 7621–7629. https://doi.org/10.1021/acs.est.8b00829.

(68) Li, F.; Duan, J.; Tian, S.; Ji, H.; Zhu, Y.; Wei, Z.; Zhao, D. Short-Chain per- and Polyfluoroalkyl Substances in Aquatic Systems: Occurrence, Impacts and Treatment. *Chemical Engineering Journal* **2020**, *380*, 122506. https://doi.org/10.1016/j.cej.2019.122506.

(69) Pan, Y.; Zhang, H.; Cui, Q.; Sheng, N.; Yeung, L. W. Y.; Guo, Y.; Sun, Y.; Dai, J. First Report on the Occurrence and Bioaccumulation of Hexafluoropropylene Oxide Trimer Acid: An Emerging Concern. *Environ. Sci. Technol.* **2017**, *51* (17), 9553–9560. https://doi.org/10.1021/acs.est.7b02259.

(70) Zhang, Y.; Lai, S.; Zhao, Z.; Liu, F.; Chen, H.; Zou, S.; Xie, Z.; Ebinghaus, R. Spatial Distribution of Perfluoroalkyl Acids in the Pearl River of Southern China. *Chemosphere* **2013**, *93* (8), 1519–1525. https://doi.org/10.1016/j.chemosphere.2013.07.060.

(71) Li, Y.; Feng, X.; Zhou, J.; Zhu, L. Occurrence and Source Apportionment of

Novel and Legacy Poly/Perfluoroalkyl Substances in Hai River Basin in China Using Receptor Models and Isomeric Fingerprints. *Water Research* **2020**, *168*, 115145. https://doi.org/10.1016/j.watres.2019.115145.

(72) Wang, R.; Zhang, J.; Yang, Y.; Chen, C.-E.; Zhang, D.; Tang, J. Emerging and Legacy Per-and Polyfluoroalkyl Substances in the Rivers of a Typical Industrialized Province of China: Spatiotemporal Variations, Mass Discharges and Ecological Risks. *Front. Environ. Sci.* **2022**, *10*, 986719. https://doi.org/10.3389/fenvs.2022.986719.

(73) Munoz, G.; Fechner, L. C.; Geneste, E.; Pardon, P.; Budzinski, H.; Labadie, P. Spatio-Temporal Dynamics of per and Polyfluoroalkyl Substances (PFASs) and Transfer to Periphytic Biofilm in an Urban River: Case-Study on the River Seine. *Environ Sci Pollut Res* **2018**, *25* (24), 23574–23582. https://doi.org/10.1007/s11356-016-8051-9.

(74) Li, H.; Zhu, X.; Zhang, J.; Wang, Z.; Li, R. Characterizing the Long-Term Occurrence and Anthropogenic Drivers of per- and Polyfluoroalkyl Substances in Surface Water of the Rhine River. *Water Research* **2023**, *245*, 120528. https://doi.org/10.1016/j.watres.2023.120528.

(75) Hong, S.; Khim, J. S.; Park, J.; Kim, M.; Kim, W.-K.; Jung, J.; Hyun, S.; Kim, J.-G.; Lee, H.; Choi, H. J.; Codling, G.; Giesy, J. P. In Situ Fate and Partitioning of Waterborne Perfluoroalkyl Acids (PFAAs) in the Youngsan and Nakdong River Estuaries of South Korea. *Science of The Total Environment* **2013**, *445–446*, 136–145. https://doi.org/10.1016/j.scitotenv.2012.12.040.

(76) Cheng, H.; Jin, H.; Lu, B.; Lv, C.; Ji, Y.; Zhang, H.; Fan, R.; Zhao, N. Emerging Poly- and Perfluoroalkyl Substances in Water and Sediment from Qiantang River-Hangzhou Bay. *Science of The Total Environment* **2023**, *875*, 162687. https://doi.org/10.1016/j.scitotenv.2023.162687.

(77) Lam, N.-H.; Cho, C.-R.; Lee, J.-S.; Soh, H.-Y.; Lee, B.-C.; Lee, J.-A.; Tatarozako, N.; Sasaki, K.; Saito, N.; Iwabuchi, K.; Kannan, K.; Cho, H.-S. Perfluorinated Alkyl Substances in Water, Sediment, Plankton and Fish from Korean Rivers and Lakes: A Nationwide Survey. *Science of The Total Environment* **2014**, *491–492*, 154–162. https://doi.org/10.1016/j.scitotenv.2014.01.045.

(78) Lam, N. H.; Cho, C.-R.; Kannan, K.; Cho, H.-S. A Nationwide Survey of Perfluorinated Alkyl Substances in Waters, Sediment and Biota Collected from Aquatic Environment in Vietnam: Distributions and Bioconcentration Profiles. *Journal of Hazardous Materials* **2017**, *323*, 116–127. https://doi.org/10.1016/j.jhazmat.2016.04.010.

(79) Bai, X.; Son, Y. Perfluoroalkyl Substances (PFAS) in Surface Water and Sediments from Two Urban Watersheds in Nevada, USA. *Science of The Total Environment* **2021**, *751*, 141622. https://doi.org/10.1016/j.scitotenv.2020.141622.

(80) Labadie, P.; Chevreuil, M. Partitioning Behaviour of Perfluorinated Alkyl Contaminants between Water, Sediment and Fish in the Orge River (Nearby Paris, France). *Environmental Pollution* **2011**, *159* (2), 391–397. https://doi.org/10.1016/j.envpol.2010.10.039.

(81) Ahrens, L.; Taniyasu, S.; Yeung, L. W. Y.; Yamashita, N.; Lam, P. K. S.; Ebinghaus, R. Distribution of Polyfluoroalkyl Compounds in Water, Suspended Particulate Matter and Sediment from Tokyo Bay, Japan. *Chemosphere* **2010**, *79* (3), 266–272. https://doi.org/10.1016/j.chemosphere.2010.01.045.

(82) Wang, S.; Ma, L.; Chen, C.; Li, Y.; Wu, Y.; Liu, Y.; Dou, Z.; Yamazaki, E.; Yamashita, N.; Lin, B.-L.; Wang, X. Occurrence and Partitioning Behavior of Per- and Polyfluoroalkyl Substances (PFASs) in Water and Sediment from the Jiulong Estuary-Xiamen Bay, China. *Chemosphere* **2020**, *238*, 124578. https://doi.org/10.1016/j.chemosphere.2019.124578.

(83) Zhao, P.; Xia, X.; Dong, J.; Xia, N.; Jiang, X.; Li, Y.; Zhu, Y. Short- and Long-Chain Perfluoroalkyl Substances in the Water, Suspended Particulate Matter, and Surface Sediment of a Turbid River. *Science of The Total Environment* **2016**, *568*, 57–65. https://doi.org/10.1016/j.scitotenv.2016.05.221.

(84) Freeling, F.; Behringer, D.; Heydel, F.; Scheurer, M.; Ternes, T. A.; Nödler, K. Trifluoroacetate in Precipitation: Deriving a Benchmark Data Set. *Environ. Sci. Technol.* **2020**, *54* (18), 11210–11219. https://doi.org/10.1021/acs.est.0c02910.

(85) Cahill, T. M. Increases in Trifluoroacetate Concentrations in Surface Waters over Two Decades. *Environ. Sci. Technol.* **2022**, *56* (13), 9428–9434. https://doi.org/10.1021/acs.est.2c01826.

(86) Lenka, S. P.; Kah, M.; Padhye, L. P. Occurrence and Fate of Poly- and Perfluoroalkyl Substances (PFAS) in Urban Waters of New Zealand. *Journal of Hazardous Materials* **2022**, *428*, 128257. https://doi.org/10.1016/j.jhazmat.2022.128257.

(87) Wu, J.; Zhuang, Y.; Dong, B.; Wang, F.; Yan, Y.; Zhang, D.; Liu, Z.; Duan, X.; Bo, Y.; Peng, L. Spatial Heterogeneity of Per- and Polyfluoroalkyl Substances Caused by Glacial Melting in Tibetan Lake Nam Co Due to Global Warming. *Journal of Hazardous Materials* **2024**, *478*, 135468. https://doi.org/10.1016/j.jhazmat.2024.135468.

(88) Gorji, S. G.; Mackie, R.; Prasad, P.; Knight, E. R.; Qu, X.; Vardy, S.; Bowles, K.; Higgins, C. P.; Thomas, K. V.; Kaserzon, S. L. Occurrence of Ultrashort-Chain PFASs in Australian Environmental Water Samples. *ENVIRONMENTAL SCIENCE & TECHNOLOGY LETTERS* **2024**, *11* (12), 1362–1369. https://doi.org/10.1021/acs.estlett.4c00750.

(89) Zhi, Y.; Lu, X.; Munoz, G.; Yeung, L. W. Y.; De Silva, A. O.; Hao, S.; He, H.; Jia, Y.; Higgins, C. P.; Zhang, C. Environmental Occurrence and Biotic Concentrations of Ultrashort-Chain Perfluoroalkyl Acids: Overlooked Global Organofluorine Contaminants. *ENVIRONMENTAL SCIENCE & TECHNOLOGY* **2024**, *58* (49), 21393–21410. https://doi.org/10.1021/acs.est.4c04453.

(90) Liu, S.; Liu, Y.; Tang, B.; Wang, Q.; Zhang, M.; Qiu, W.; Luo, X.; Mai, B.; Hao, Y.; Zheng, J.; Wang, K.; Wang, D. Spatial Distribution, Trophic Magnification, and Risk Assessment of per- and Polyfluoroalkyl Substances in Yangtze Finless Porpoise (Neophocaena Asiaeorientalis Asiaeorientalis): Risks of Emerging Alternatives. *JOURNAL OF HAZARDOUS MATERIALS* **2024**, *477*. https://doi.org/10.1016/j.jhazmat.2024.135246.

(91) Mo, L.; Wan, N.; Zhou, B.; Shao, M.; Zhang, X.; Li, M.; Liu, Y.; Mai, B. Per- and Polyfluoroalkyl Substances in Waterbird Feathers around Poyang Lake, China: Compound and Species-Specific Bioaccumulation. *ECOTOXICOLOGY AND ENVIRONMENTAL SAFETY* **2024**, *273*. https://doi.org/10.1016/j.ecoenv.2024.116141.

(92) Tang, A.; Zhang, X.; Li, R.; Tu, W.; Guo, H.; Zhang, Y.; Li, Z.; Liu, Y.; Mai, B. Spatiotemporal Distribution, Partitioning Behavior and Flux of per- and Polyfluoroalkyl Substances in Surface Water and Sediment from Poyang Lake, China. *CHEMOSPHERE* **2022**, *295*. https://doi.org/10.1016/j.chemosphere.2022.133855.

753 **Table 1.** Mean, maximum and minimum concentrations and detection frequency (DF) of PFAS in

754 water and sediment.

	Water (ng/L)				Sediment (ng/g dw)			
	min	max	mean	DF	min	max	mean	DF
PFBA	0.56	100	8.5	100%	<LOQ	2.6	0.36	38%
PFPeA	<LOQ	7.1	1.6	91%	<LOQ	0.03	0.04	10%
PFHxA	<LOQ	46	5.2	99%	<LOQ	3.3	0.15	35%
PFHpA	<LOQ	3.9	0.39	38%	<LOQ	0.91	0.10	46%
PFOA	<LOQ	140	13	97%	<LOQ	1.1	0.03	59%
PFNA	<LOQ	7.8	0.36	60%	<LOQ	0.11	0.11	27%
PFDA	<LOQ	2.8	<LOQ	9%	<LOQ	0.12	0.04	39%
PFUnDA	<LOQ	<LOQ	<LOQ	0%	<LOQ	0.19	0.08	48%
PFDoDA	<LOQ	1.2	<LOQ	1%	<LOQ	0.08	0.05	83%
PFTriA	<LOQ	0.28	<LOQ	1%	<LOQ	0.03	0.02	1%
PFTreA	<LOQ	0.35	<LOQ	1%	<LOQ	<LOQ	<LOQ	0%
PFBS	0.14	160	18	100%	<LOQ	1.6	0.02	93%
PFPeS	<LOQ	3.6	0.22	70%	<LOQ	0.17	0.02	69%
PFHxS	<LOQ	4.9	0.67	93%	<LOQ	0.53	1.7	69%
PFHpS	<LOQ	2.2	0.24	78%	<LOQ	0.21	0.03	93%
PFOS	<LOQ	12	1.2	99%	<LOQ	0.50	0.02	59%
PFNS	<LOQ	5.4	0.21	79%	<LOQ	0.11	0.01	79%
HFPO-DA	<LOQ	1.3	<LOQ	14%	<LOQ	0.02	0.01	20%
HFPO-TA	<LOQ	18	2.5	96%	<LOQ	4.8	0.26	77%
FBSA	<LOQ	110	4.4	83%	<LOQ	0.22	0.02	13%
FHxSA	<LOQ	4.2	0.14	76%	<LOQ	0.020	<LOQ	1%
FOSA	<LOQ	2.5	0.13	90%	<LOQ	3.64	<LOQ	73%
PFECHS	<LOQ	0.38	0.04	43%	<LOQ	0.01	<LOQ	8%
4:2 FTSA	<LOQ	19	0.99	96%	<LOQ	0.17	0.03	63%
6:2 FTSA	<LOQ	1.7	0.10	68%	<LOQ	0.16	0.02	70%
8:2 FTSA	<LOQ	0.16	<LOQ	41%	<LOQ	3.1	0.28	51%
6:2 FTCA	<LOQ	2.7	<LOQ	22%	<LOQ	0.38	0.02	8%
8:2 FTCA	<LOQ	18	0.66	55%	<LOQ	2.4	0.08	35%
10:2 FTCA	<LOQ	6.5	0.36	24%	<LOQ	1.7	0.02	1%
6:2 Cl-PFESA	<LOQ	1.4	0.08	74%	<LOQ	0.13	0.02	41%
8:2 Cl-PFESA	<LOQ	0.50	0.02	11%	<LOQ	0.03	0.01	21%
ΣPFAS	5.5	340	58		0.19	30	4.0	

755 LOQ: Limit of quantification.

Table 2 Site name, CD, QW, FD, CSPM, C′, QS, FS and Contribution of suspended matter of PFAS in dissolved phase and particle phase in dry and flood seasons.

	Site name	C_D (ng/L)	Q_W (10^9 m^3)	F_D (kg/month)	C_{SPM} (ng/g)	C' (g/L)	Q_S (10^4 t)	F_S (kg/month)	Contribution of suspended matter
Dry season	CJ2	48	130	620.0	18	0.0164	20.0	220	26%
	CJ11	32	280	880.0	0.39	0.0008	10.0	49	5%
	CJ13	39	260	1100	0.58	0.0073	30.0	24	2%
	CJ16	26	470	1200	7.5	0.0399	280	520	30%
	CJ18	42	670	2800	-	-	-	-	-
	CJ25	81	540	4400	7.7	0.0464	420	690	14%
	DTH1	92	200	1800	7.7	0.0082	160	1500	45%
	PYH1	339	190	6400	0.08	0.0305	100	2.5	<1%
Flood season	CJ2	17	230	400.0	16	0.013	20.0	240	38%
	CJ3	7.5	320	240.0	4.4	0.013	200	99	29%
	CJ13	28	380	1100	0.83	0.0079	65.0	68	6%
	CJ16	32	500	1600	1.3	0.031	400	170	10%
	CJ21	67	670	4500	-	-	-	-	-
	CJ25	58	660	3800	0.65	0.0392	400	66	2%
	CJ53	73	710	5300	-	-	-	-	-
	DTH1	21	97.0	200.0	1.7	0.0403	80.0	34	15%
	PYH1	47	57.0	270.0	0.44	0.0279	20.0	3.1	1%
	JSJ1	13	120	150.0	0.12	0.0059	6.00	1.3	1%
	JSJ3	6.6	70.0	78.00	1.1	0.0149	8.00	5.7	7%
	HJ1	16	620	970.0	0.61	0.0096	590	380	28%
	MJ1	32	80.0	250.0	0.46	0.0209	10.0	2.2	1%
	JLJ2	5.4	81.0	44.00	0.32	0.0367	40.0	3.5	7%
	WJ1	11	39.0	41.00	1.33	0.0061	17.0	37	47%

"-": No data available. ADD THE DEFINTIONS OF CD, QW ETC ETC?

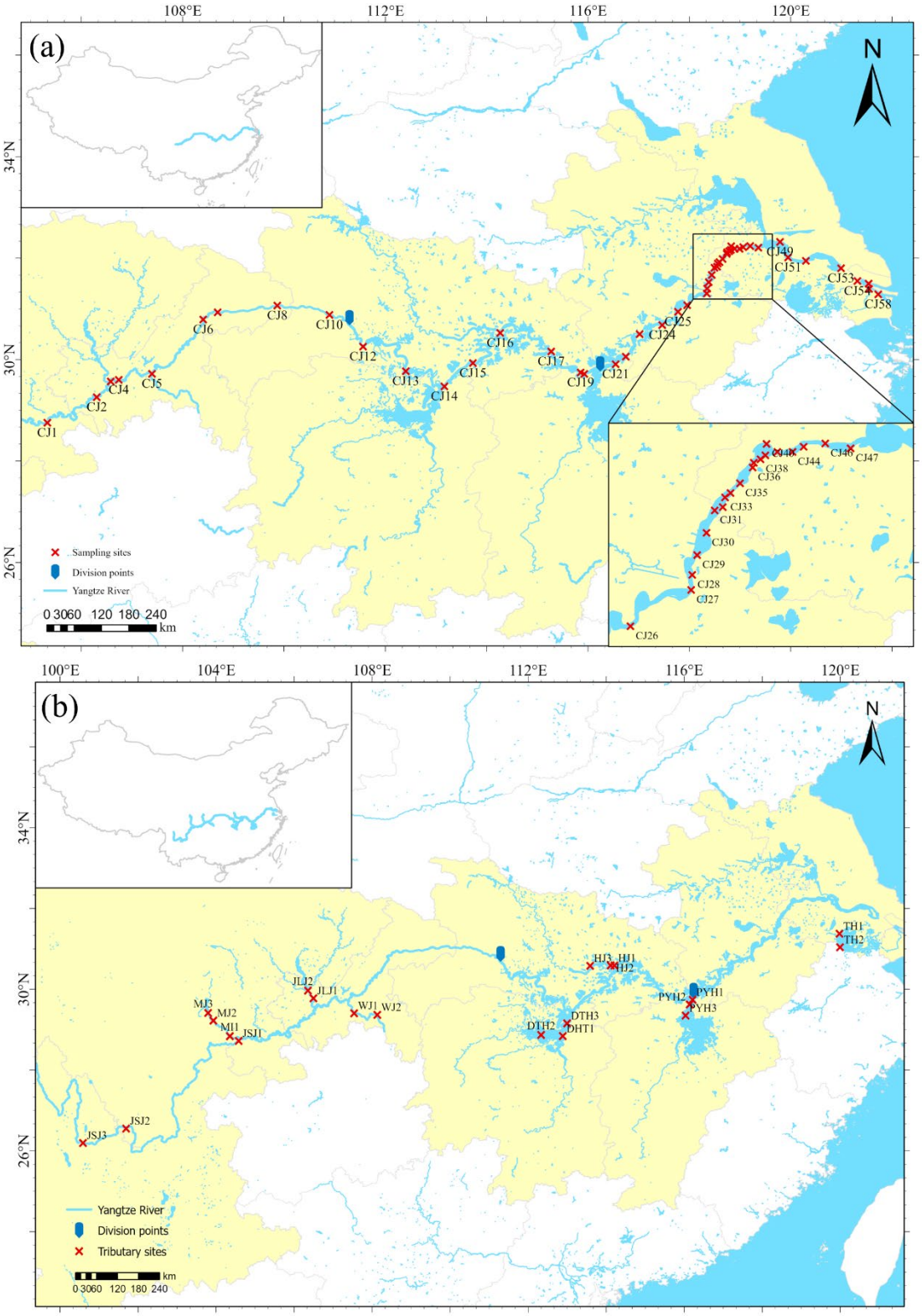

Figure 1 Map of the sampling sites (a: Sampling sites in the mainstream of the Yangtze River; b: Sampling sites in the Jinshajiang River, four tributaries and three lakes).

763

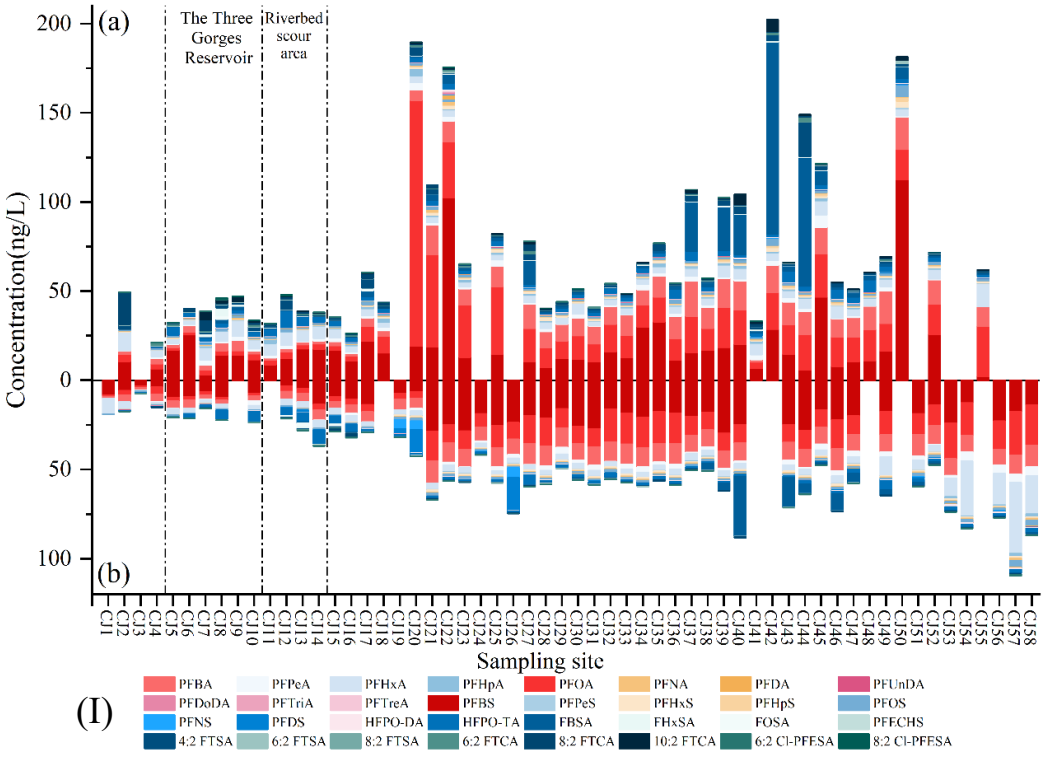

764

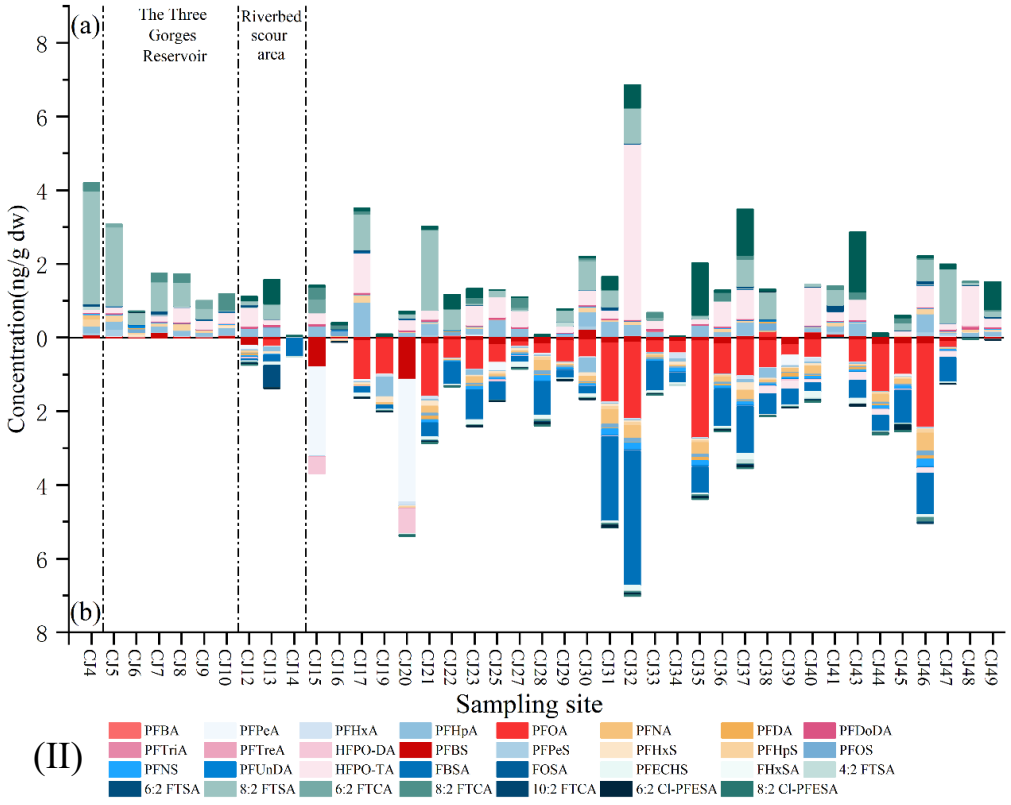

765 **Figure 2** PFAS concentrations in water (ng/L) and sediment (ng/g dw) at individual sites in dry (a)
766 and flood (b) season. Samples were collected (I: water; II: sediment, concentrations shown aszero
767 in the figure mean no sample was collected).

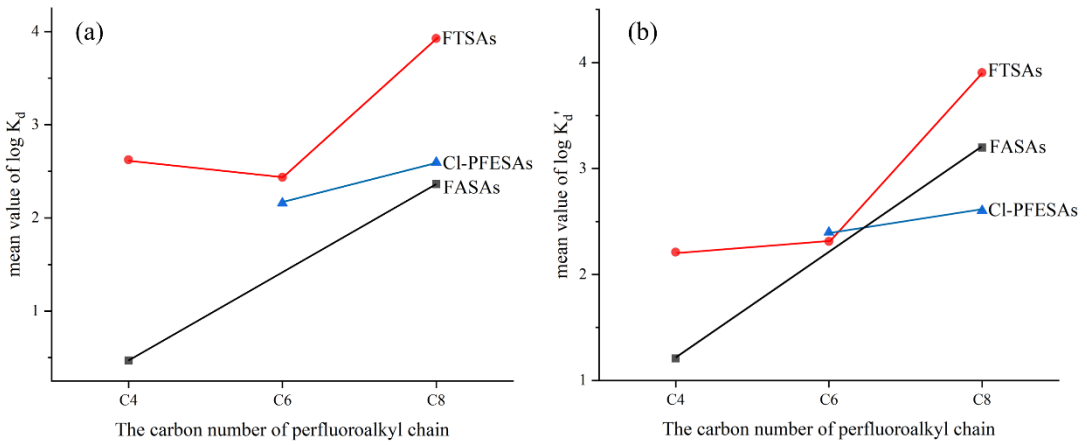

768

769 **Figure 3** The log K_d and K_d'values of FTSAs, FASAs, and Cl-PFESAs (a: Partition coefficients

770 for dissolved and particle phases; b: Partition coefficients for sediment and dissolved phase).

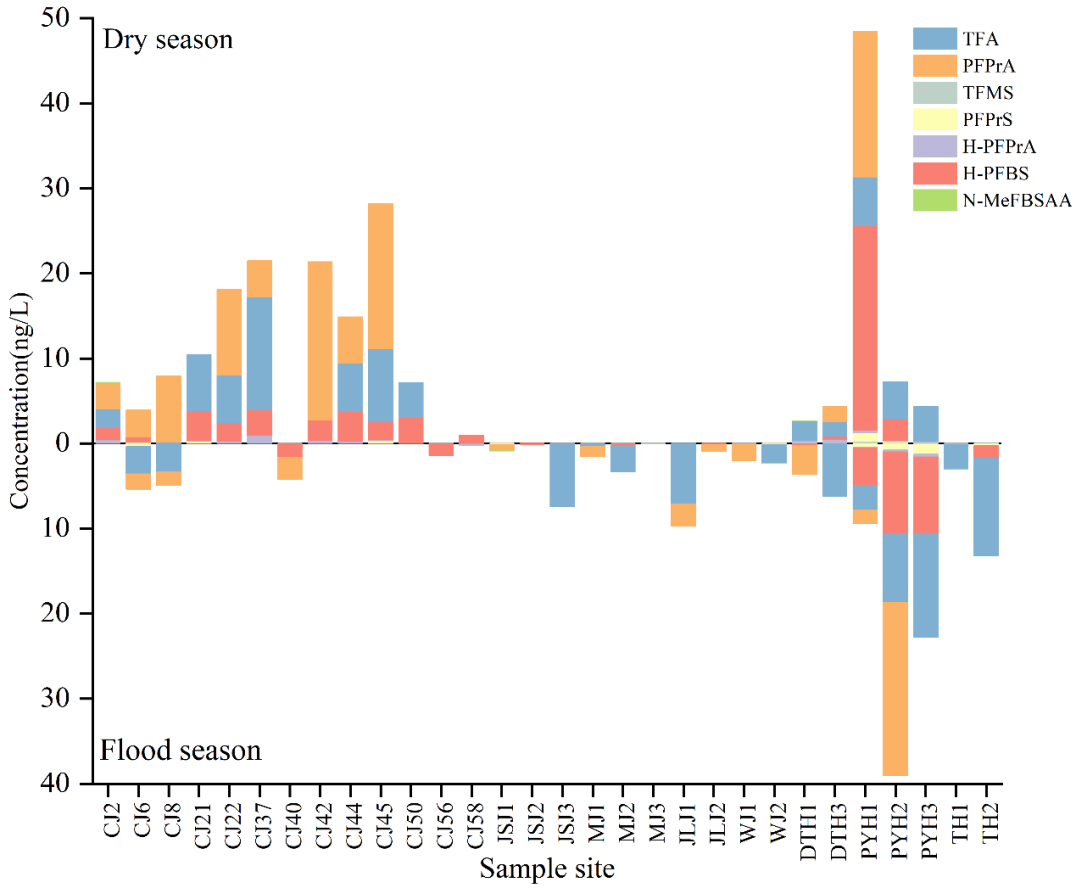

771

772 **Figure 4** The raw semi-quantitative data for 38 samples (concentrations shown as zero in the

773 figure means no sample was collected).